

See discussions, stats, and author profiles for this publication at: <https://www.researchgate.net/publication/222090760>

Cavity dispersion tuning spectroscopy of tellurium near 444.4 nm

Article in *Journal of the Optical Society of America B* · December 2011

DOI: 10.1364/JOSAB.28.002934

CITATIONS

3

READS

109

7 authors, including:



Haoquan Fan

University of Maryland, College Park

21 PUBLICATIONS 332 CITATIONS

[SEE PROFILE](#)



Pramudith Rupasinghe

Sri Lanka Red Cross Society

12 PUBLICATIONS 42 CITATIONS

[SEE PROFILE](#)



Tao Yang

University of Hawai'i at Mānoa

64 PUBLICATIONS 237 CITATIONS

[SEE PROFILE](#)



Neil Shafer-Ray

University of Oklahoma

66 PUBLICATIONS 1,198 CITATIONS

[SEE PROFILE](#)

Some of the authors of this publication are also working on these related projects:



quantum memory with rare-earth ion-doped crystals. [View project](#)



Rydberg-atom based radio-frequency electrometry using frequency modulation spectroscopy in room temperature vapor cells [View project](#)

Cavity dispersion tuning spectroscopy of tellurium near 444.4 nm

James Coker, Haoquan Fan, C. P. McRaven, P. M. Rupasinghe, T. Zh. Yang, N. E. Shafer-Ray,* and J. E. Furneaux

Department of Physics and Astronomy, The University of Oklahoma, 440 W. Brooks St., Norman, Oklahoma 73072, USA

**Corresponding author: shaferry@nhn.ou.edu*

Received August 2, 2011; revised October 3, 2011; accepted October 9, 2011; posted October 18, 2011 (Doc. ID 151919); published November 17, 2011

We present saturation absorption spectroscopy of transitions in Te_2 near 444.4 nm. These spectra were taken using a blue diode laser locked to a Fabry–Perot (FP) cavity that is in turn locked to a Zeeman-stabilized helium–neon laser. Tuning of the diode laser frequency is accomplished by N_2 pressure tuning of the FP cavity. The result is a tuning frequency that is proportional to the dispersion of the index of refraction between the helium neon and diode laser wavelengths. We assess the stability of the blue laser frequency by scanning over a single Te_2 absorption line repeatedly over a 48 h period. This work is motivated by our desire to produce a versatile frequency-locked source of radiation for use in molecular optical polarization experiments. © 2011 Optical Society of America

OCIS codes: 120.6200, 140.3425, 300.6260, 300.6320.

1. INTRODUCTION

The diode laser has been a valuable research tool since the 1960s [1,2]. Though it has been used for countless experiments over the decades, many applications require frequency stability beyond that provided by typical commercial mode-locked systems. An unaided, research-grade diode laser typically drifts from several megahertz per minute to a few megahertz per hour [3]. A handful of techniques have arisen over the years to improve the frequency stability of diode lasers.

One method is to feedback stabilize the laser frequency to an atomic absorption or fluorescence line. For example, the setup of [4] used a GaAlAs laser, with a 3.0 kHz frequency modulation, to create fluorescence from a well-known transition in cesium. If the laser were tuned slightly below the peak (to the red), then the 3.0 kHz modulation would be seen in the fluorescence signal, in phase with the modulation that was written on the laser. If the laser were tuned slightly above the peak (to the blue), then the 3.0 kHz modulation would be seen in the fluorescence signal with opposite phase. By use of a lock-in amplifier, an error signal was generated, appropriately amplified, and fed back to the current controller of the laser diode. With this setup, a frequency drift of <50 kHz was demonstrated. While the improvement of frequency stability by three to five orders of magnitude is impressive, the experimenter is limited by having to lock at a specific, well-known transition.

Without reference to a known transition, frequency-stabilizing lasers to a drift of one part in 10^{14} has been demonstrated by locking to ultralow expansion cavities [5]. To enable the laser to reliably shift in frequency, one may instead lock a sideband of the beam to a cavity and scan the modulation frequency of the sideband [6]. While this method is highly stable, its scanning range is limited by how fast one can modulate the sideband, (~ 100 MHz). Other methods of frequency

stabilizing diode lasers without reference to a known transition, utilizing optical transfer cavities, write the stability of one laser onto another [7–15]. The scanning transfer cavity stabilizes the difference in transmission peaks of the reference laser and target laser as the cavity sweeps back and forth, using feedback electronics [9–11,15]. Although a long-term frequency drift on the order of a few MHz has been demonstrated [10], the duty cycle for feedback is of the order of the cavity finesse ($\sim 1/100$), which limits the short-term frequency stabilization of the lock.

Making the transmission peaks of the two lasers coincide removes the requirement of sweeping the cavity and thus improves the short-term stability. This has been done by frequency shifting either laser with an electro-optic modulator (EOM) [12,13]. For broad tunability, it is required to have broadband-capable modulators, and continuous scans are limited to half the cavity's free spectral range (FSR). One may avoid using an EOM by radiofrequency current modulation in the target laser diode [8], but this requires a laser system that is capable of modulation at such speeds and still has a scanning range that depends on the cavity's FSR. Further, increasing the cavity's FSR spaces apart from potential locking points, but decreasing the cavity's FSR can shorten the scanning range.

We present an alternative stabilization technique in which both lasers are resonant with the transfer cavity but neither optical modulation nor current modulation of the laser diode is required. By dispersion tuning the cavity, it can be made resonant with both lasers simultaneously at arbitrary frequencies, and by dispersion tuning while the cavity is locked, the target laser can be scanned while possessing the stability of the reference laser. We demonstrate this setup by measuring Lorentzian line profiles and line spacings of optical transitions in molecular tellurium (Te_2) by saturation absorption

spectroscopy. We discuss stability with time and temperature, and comment on the dispersions of various gases.

2. EXPERIMENTAL SETUP

The setup is described as three separate parts: the laser system, the physical principles of the locking and scanning system, and the optical setup for observation of saturated absorption lines in Te_2 .

A. Laser Locking System

The laser setup is depicted in Fig. 1. The Zeeman-stabilized helium–neon (He–Ne) laser (MicroGauss) is used as a reference for both a Wavemeter (Burleigh WA-1000) and a confocal Fabry–Perot (FP) Etalon (Toptica FPI 100-500-3V0). The blue diode laser (Toptica TA SHG Pro) makes its 440 nm light by doubling 880 nm IR light in a bow-tie cavity with a beta-barium-borate crystal. We control the frequency of the IR diode using the analog interface to the Toptica DC110 control system. This frequency is measured with the wavemeter, as shown in Fig. 1. The blue output is about 280 mW. Dichroic beam splitters are used to direct $\sim 30\%$ of this power to a Te_2 absorption cell and $\sim 1\%$ to the etalon. The etalon temperature is controlled using a heater, and the etalon pressure is controlled using a stepper motor attached to bellows. The precision of pressure control with the stepper motor system far surpasses the precision of the pressure gauge. The length of the etalon is controlled by shifting one of the mirrors with a piezoelectric transducer (PZT).

A combination of dichroic beam splitters and filter glass at the output of the etalon enables independent detection of the red and blue light at separate photodiodes. These signals are used for the electronic feedback loops. In contrast to the scanning transfer cavity system [15], for the duration of its lock, the FP cavity is continuously in resonance with both lasers. To achieve double resonance, we allow the cavity to sweep while adjusting the pressure inside until both lasers are resonant, then lock up both the cavity to the reference laser and the target laser to the cavity. For scanning, the FP cavity optical path is maintained in resonance with the He–Ne laser as the index of refraction of the N_2 gas changes by adjusting the PZT on one of the mirrors. The mirror position is modulated at 5 kHz. If the response on the He–Ne photodiode is in phase, the cavity is shortened; if the response is 180° out of phase, the cavity is lengthened. The 5 kHz modulation and the error

signal are added together in a transformer and applied to the PZT. This same modulation of the FP cavity also affects the reading from the blue laser's photodiode. This is similarly used to adjust the diode laser's frequency to maintain resonance with the FP cavity. This frequency is tuned by adjusting the grating and current of the diode laser system using the feed-forward grating control of the Toptica system.

Low pass filters are used for each of the error signals, and the optimal cutoff frequencies empirically found for each give a good estimate of the bandwidth of each lock. The cavity's lock to the reference laser is ~ 500 Hz, and that of the diode laser's lock to the cavity is ~ 50 Hz. The short-term stability of the reference He–Ne laser is reported by its documentation to be < 100 kHz. Here follows the theory of the locking system and dispersion tuning technique.

B. Physics of Cavity Dispersion Tuning (CDT) Spectroscopy

By locking the cavity length L to the He–Ne reference laser wavelength λ_R , we set

$$L = \frac{\lambda_R}{2}(N_R + \delta_R) = \frac{c}{2\nu_R n_R} N'_R \quad (1)$$

for some fixed integer N_R , where ν_R and n_R are the frequency and index of refraction of the reference laser and c is the speed of light. The δ_R represents the Gouy phase, the added phase due to reflections, and the wavelength-dependent phase shift induced by the cavity mirror coatings. This constant shift is absorbed into N'_R and does not affect our end result. By locking the blue diode laser vacuum wavelength λ to the cavity, the diode laser wavelength is set to

$$L = \frac{\lambda}{2}(N + \delta) = \frac{c}{2\nu n} N' \quad (2)$$

for some fixed integer N , where ν and n are the frequency and index of refraction of the blue laser, and N' is fixed at $N + \delta$. The lock condition is therefore given by

$$\frac{n\nu}{n_R\nu_R} = \frac{N'_R}{N'} = \text{A constant.} \quad (3)$$

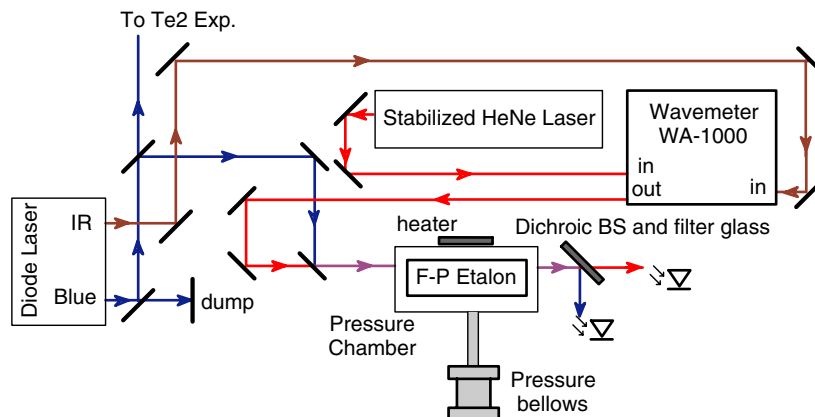


Fig. 1. (Color online) Laser locking system. The FP etalon is fixed inside a pressure chamber. Both the He–Ne laser and the blue diode laser are resonant with the etalon, and, after filtering optics, each one is seen on its own photodiode.

The frequency ν changes to maintain this condition as n and n_R are altered. The etalon is filled with nitrogen (N_2) gas, and the temperature T and pressure P are controlled with a heater and bellows as mentioned earlier. At fixed $P_0 = 760$ torr and $T_0 = 15^\circ\text{C}$, the index of refraction for different colors of visible light has been well characterized [16]:

$$n(P_0, T_0) - 1 = \left(6497.378 + \frac{3073864.9}{144 - k^2} \right) / 10^8 \equiv \alpha_0(k), \quad (4)$$

where k is the wavenumber of light in inverse microns. The values for the reference He-Ne laser at 632.8 nm and the blue diode laser at 444.4 nm are $\alpha_0(k_R) = 2.8220 \times 10^{-4}$ and $\alpha_0(k) = 2.8622 \times 10^{-4}$, respectively. The index of refraction at a pressure and temperature (P_f, T_f) may be related to the index of refraction at (P_i, T_i) by the expression

$$\alpha_f(k) = \alpha_i(k) \Gamma_i^f, \quad (5)$$

where, from [17],

$$\Gamma_i^f = \frac{(P_f/T_f)Z_i}{(P_i/T_i)Z_f + \alpha_i Z_i (P_i/T_i - P_f/T_f)/6} \approx \frac{P_f}{T_f} / \frac{P_i}{T_i} \quad (6)$$

with

$$Z = 1 + \frac{P(T - 317.6 \text{ K}) \times 10^{-5}}{760 \text{ torr}} \quad (7)$$

being the compressibility of Nitrogen at a given (P, T) . Note that the approximation in Eq. (6) was not used in our analysis, but is included to aid the reader's intuition.

With $n\nu/n_R\nu_R$ a constant of the lock [Eq. (3)], we derive an expression for the change in frequency of the tuned laser as the pressure and temperature are changed from P_i, T_i to P_f, T_f :

$$\Delta\nu_i^f = \frac{(\Gamma_0^f - \Gamma_0^i)(\alpha_0(k_R) - \alpha_0(k))}{(1 + \alpha_0(k_R)\Gamma_0^i)(1 + \Gamma_0^f\alpha_0(k))} \nu_i. \quad (8)$$

Here the subscript 0 denotes the (P, T) conditions where the α s were measured in [16] and the i s denote chosen reference frequency conditions. The frequency scanning range for a given pressure range thus depends on the difference in frequencies of the reference and target lasers. Figure 2 shows a plot of Eq. (8) over roughly 3 atm and with a variety of target laser

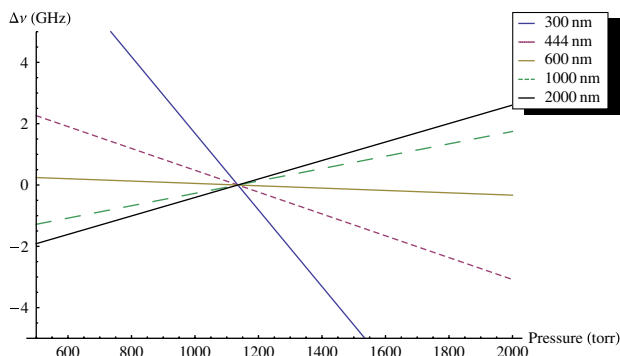


Fig. 2. (Color online) Plot of Eq. (8) spanning roughly 3 atm of pressure for fixed $T = 15^\circ\text{C}$ and $\nu_R = 632.8$ nm.

frequencies. The scanning range is largest when ν is far from and less than ν_R , but even at $\nu = 600$ nm, the scanning range is over 1 GHz.

In practice, Eq. (8) cannot be used to the level of precision implied without very precise knowledge of the gas purity and the cavity pressure. The method used to compensate for this is discussed in Subsection 3.B.

C. Remarks on Dispersion of Various Gases

Originally, we attempted to use carbon dioxide (CO_2) gas for dispersion scanning, which would have allowed for a larger frequency scanning range [18], but found that the temperature stability required for CO_2 was beyond our reach. We estimate the temperature dependence of $\Delta\nu$, using data from [19] applied to Eq. (8), to be nearly 1 GHz/ $^\circ\text{C}$. This is due to the fact that CO_2 is nearer to a phase transition than N_2 is at these P, T conditions, and somewhat due to the fact that CO_2 is more dispersive at the wavelengths used. In contrast, argon gas was considered, but we found too small a dispersion in this region [20].

D. Optical Setup for Saturation Absorption Spectroscopy of Tellurium

The optical setup surrounding the tellurium cell is illustrated in Fig. 3. Continuing from Fig. 1, the blue diode laser goes through a half-wave plate and a polarizing beam splitter (PBS), splitting the beam in two, with the ratio of powers controllable by rotating the half-wave plate. The undeflected and deflected beams will be referred to as the pump and probe beams, respectively. The pump beam's intensity is made to oscillate by the electro-optical amplitude modulator, which, in combination with wave plates B and C and the second PBS, creates an electro-optical chopper. The pump beam passes through the third PBS and is then detected by the photodiode. The probe beam is bent by all three PBSs and detected by the other photodiode in the diagram. For the moment, we will ignore the electrical-optical modulator (EOM), as it was only used for part of the experiment described later in this paper.

The modulation source and the probe photodiode signal are fed into a lock-in amplifier. While tuned to a tellurium line, the modulation of the pump beam becomes written on the probe beam. At a moment when the pump beam is of high intensity, a hole in the population is made, allowing more of the probe beam to pass. At a moment when the pump beam is of low intensity, the probe beam absorbs, allowing less of the probe beam to pass. The ideal modulation frequency should be set high to optimize the signal to noise ratio, but not high enough to be comparable to collision broadening lifetimes, thus distorting relative peak intensities. We used a 40 kHz modulation.

3. DATA

All peaks observed are from various rovibrational transitions in the $X_1(^3\Sigma_g^-) \leftarrow B_1(^3\Sigma_u^-)$ band, previously assigned line numbers in [21].

A. Preliminary Grating Scan

Before performing dispersion scans, a scan of the PZT voltage on the diode laser's grating was performed, which spanned about 25 GHz. While scanning the grating, the etalon was locked to the He-Ne laser, the blue diode laser was not locked, and its intensity through the etalon was recorded.

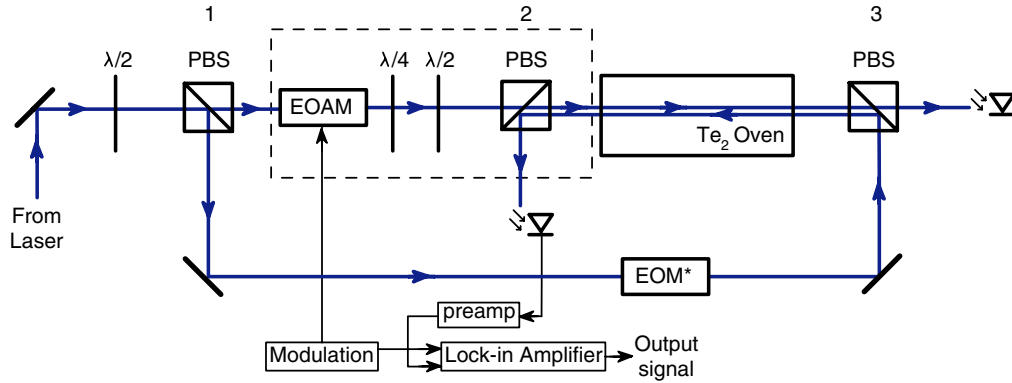


Fig. 3. (Color online) Optics surrounding the tellurium cell, which is held at 650 °C. The dashed box groups together the components that serve as an electro-optical chopper.

Spikes in intensity occurred when the frequency of the blue laser was resonant with the etalon, and they provided markers that indicated one FSR in frequency. Our confocal etalon has a finesse of ~ 200 and is designed such that $\text{FSR} = 1 \text{ GHz}$, accurate to 1%. By adjusting the alignment into the etalon, we increased the relative amplitude of every other spike, making the $c/2nL$ cavity modes more intense than the $c/4nL$ modes. As the laser sweeps, its pointing alignment also shifts slightly, which changes the coupling to the etalon leading to further intensity variations in the modes. Our wavemeter was calibrated by an unrelated Rubidium experiment in a nearby lab, and found to be accurate to $<1 \text{ GHz}$. This scan is shown in Fig. 4.

The built-in Toptica system used for scanning the grating uses a feed-forward method that adjusts the current as the grating is shifted in order to maintain an ideal gain curve at each grating position. Because stable scanning of the diode laser grating over a long frequency range requires adjustment of the diode current, the scan is nonlinear in frequency. After analysis, fitting a quadratic function to the gigahertz markers and rescaling, we can determine the intervals between lines to an uncertainty of 50 MHz. In matching our lines to [21], we define our line matching their line 1525 to be zero Hz and report the intervals measured in Table 1. We have FWHM values around 15 MHz, compared to the 3 GHz values of the previous work, so it is no surprise that we find 13 lines in the space where five were reported in [21].

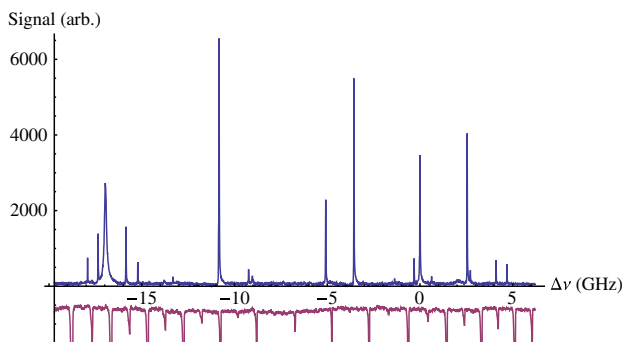


Fig. 4. (Color online) Preliminary diode laser grating scan, accurate to 50 MHz. The downward spikes are 1 GHz “markers” seen through the etalon. The alignment was set such that every other marker was diminished in amplitude.

B. CDT Scan

A CDT scan consists of collection of saturated absorption spectra while regulating the cavity temperature to $\Delta T < 0.03 \text{ }^\circ\text{C}$ and scanning the pressure by changing the volume of the closed chamber with a stepper motor driven bellows system. In principle, the frequency shift of each pressure point can be determined from Eq. (8), but, as mentioned earlier, not to that level of precision. For this reason, 40.00000 MHz sidebands were added to the probe beam in some of the scans, using the EOM shown in Fig. 3. These sidebands were then used to create an effective frequency calibration by forcing the corresponding fit-peak centers to be 40 MHz apart during fit model analysis. The ν versus P relationship measured this way was found to be consistently linear, deviating from scan to scan at most by 1%. The intensity of the diode laser through the FP cavity was monitored as data was taken to confirm that the laser never lost lock. The intensity of the pump beam was also monitored, and its fluctuations were found to be $<10\%$.

Dispersion scanning was carried out for the two peaks near line 1525. The data indicates an interval of $289 \pm 3 \text{ MHz}$, as seen in Table 1 and in Fig. 5. The uncertainty of 3 MHz comes from the linear fit used, which includes the uncertainty from the pressure gauge reading and errors due to nonparallelism

Table 1. Our Reported Intervals and Those of [21]^a

Line Position and Previous Assignment from [21] (GHz)	Interval from Line 1525 Found in This Work (GHz)
674594.113 [1522]	-17.92
	-17.36
	-16.97
	-15.85
	-15.21
674600.346 [1523]	-10.83
674607.751 [1524]	-5.08
	-3.56
674611.022 [1525]	-0.289 ± 0.003
	0
674613.621 [1526]	2.54
	4.10
	4.69

^aAll nonzero intervals have an uncertainty of 50 MHz, except the one that specifies $\pm 3 \text{ MHz}$, which was measured using dispersion tuning and sideband modulation, as described in Subsection 3.B.

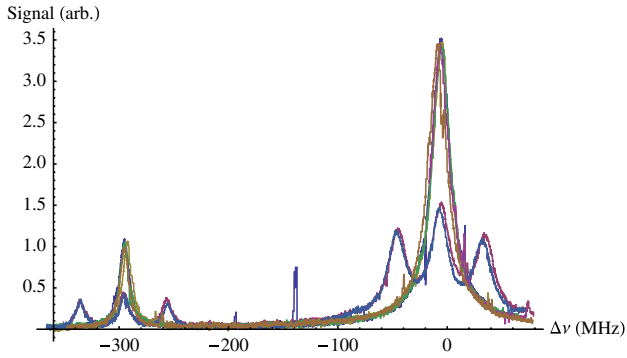


Fig. 5. (Color online) Seven CDT scans of two lines, taken over a period of two days. Some data sets include 4000000 MHz sidebands. The x axis of this scan comes directly from Eq. (8).

of the pump and probe beams. The uncertainty in the temperature reading is insignificant in comparison to that of the pressure reading. The FWHM values of the lines at -289 and 0 MHz measure 11 and 20 MHz, respectively. The peaks have Lorentzian shape, consistent with Doppler-free spectroscopy [22].

During CDT scans, the feedback output to the PZT voltage for the grating was monitored. This signal, from a typical scan converted to frequency, is shown in Fig. 6. As mentioned above, the Toptica current feed-forward system used to maximize the gain curve causes nonlinearity in the relationship between frequency and grating PZT voltage. The nonlinearity seen in the figure shows the limitation of using a grating scan to obtain a line profile from a signal that may require accurate scanning over a small range in frequency. This nonlinearity depends both on grating position and diode current, and thus it changes from day to day and even during a sweep if the diode current is adjusted for better laser stability.

In addition to the CDT scans, we tested temperature dependence of $\Delta\nu$. This was done by locking the system on the side of line 1525, then heating and cooling the etalon in a closed volume so that P/T was constant, over a few hours while monitoring the signal intensity. We found the dependence to be 20 MHz/ $^{\circ}\text{C}$, so appropriate regulation of temperature in the etalon is required.

To measure frequency drift of the blue laser, we defined the center from the Lorentzian fit of line 1525 from one data set to be 0 Hz, and then determined the fits' centers of all other data sets relative to it. In doing this over data sets that spanned

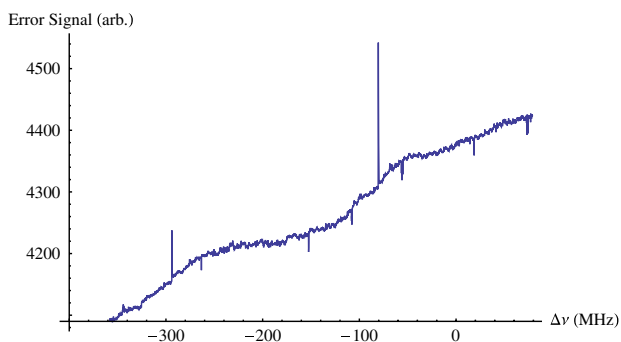


Fig. 6. (Color online) Diode grating position at each point during a typical CDT scan. At this scale, one can see that a grating scan is quite nonlinear in frequency.

a 48 h time period, we found a drift <2 MHz, thus observing a frequency stability of $\delta\nu/\nu_0 \sim 1 \times 10^{-9}$ over two days.

4. CONCLUDING REMARKS

We find that CDT spectroscopy allows laser locking at any frequency, with a drift less than 2 MHz over days, and we demonstrate a scanning range of nearly 500 MHz. We remark that this scanning range can easily be much larger, being that, in our case, we were limited simply by how far the PZT on the cavity mirror could move to follow the reference laser. This technique has merits similar to those of the nonscanning transfer cavity of [8]. While that method may be easier to implement for laser systems that are injection-locked, CDT scanning may be easier to implement for other lasers, such as the one used in this experiment. We report 11 intervals in Te_2 lines near 444.4 nm with 50 MHz uncertainty with a grating scan, and we demonstrate CDT spectroscopy in reporting one interval with 3 MHz uncertainty. The uncertainty in our measurements is consistent with the ~ 1 torr uncertainty of the pressure gauge used (MKS 122BA-10000BB). A more accurate pressure gauge would likely decrease our uncertainty, but pressure gauges with accuracy better than 0.1% are not common in this range of pressure. Manufacturers like MKS Instruments and Dwyer have some available for similar pressure ranges though, such as the MKS Type 690.

This technique may prove useful for studies where short, precise scans or locking to an arbitrary optical frequency are desired such as studies of line profiles, optical polarization experiments, or studies of molecular species with low data collection rates.

ACKNOWLEDGMENTS

This work was funded by the National Science Foundation (NSF) (NSF-0855431).

REFERENCES

1. R. N. Hall, G. E. Fenner, J. D. Kingsley, T. J. Soltys, and R. O. Carlson, "Coherent light emission from GaAs junctions," *Phys. Rev. Lett.* **9**, 366–368 (1962).
2. M. I. Nathan, W. P. Dumke, G. Burns, F. H. Dill Jr., and G. Lasher, "Stimulated emission of radiation from GaAs p-n junctions," *Appl. Phys. Lett.* **1**, 62–64 (1962).
3. C. Bradley, J. Chen, and R. G. Hulet, "Instrumentation for the stable operation of laser diodes," *Rev. Sci. Instrum.* **61**, 2097–2101 (1990).
4. D. Wang, L. Xie, and Y. Wang, "GaAlAs laser diode frequency locked at the D_2 line of Cs atoms in an atomic beam," *Opt. Lett.* **13**, 820–822 (1988).
5. P. Gill, "Optical frequency standards," *Metrologia* **42**, S125–S137 (2005).
6. J. I. Thorpe, K. Numata, and J. Livas, "Laser frequency stabilization and control through offset sideband locking to optical cavities," *Opt. Express* **16**, 15980–15990 (2008).
7. E. Riedle, S. H. Ashworth, J. J. T. Farrell Jr., and D. J. Nesbitt, "Stabilization and precise calibration of a continuous-wave difference frequency spectrometer by use of a simple transfer cavity," *Rev. Sci. Instrum.* **65**, 42–48 (1994).
8. P. Bohlouli-Zanjani, K. Afrousheh, and J. D. D. Martin, "Optical transfer cavity stabilization using current-modulated injection-locked diode lasers," *Rev. Sci. Instrum.* **77**, 093105–093109 (2006).
9. B. G. Lindsay, K. A. Smith, and F. B. Dunning, "Control of long-term output frequency drift in commercial dye lasers," *Rev. Sci. Instrum.* **62**, 1656–1657 (1991).

10. W. Z. Zhao, J. E. Simsarian, L. A. Orozco, and G. D. Sprouse, "A computer-based digital feedback control of frequency drift of multiple lasers," *Rev. Sci. Instrum.* **69**, 3737–3740 (1998).
11. A. Rossi, V. Biancalana, B. Mai, and L. Tomassetti, "Long-term drift laser frequency stabilization using purely optical reference," *Rev. Sci. Instrum.* **73**, 2544–2548 (2002).
12. B. Burghardt, W. Jitschin, and G. Meisel, "Precise rf tuning for cw dye lasers," *Appl. Phys.* **20**, 141–146 (1979).
13. D. F. Plusquellic, O. Votava, and D. J. Nesbitt, "Absolute frequency stabilization of an injection-seeded optical parametric oscillator," *Appl. Opt.* **35**, 1464–1472 (1996).
14. J. Helmcke, S. A. Lee, and J. L. Hall, "Dye laser spectrometer for ultrahigh spectral resolution: design and performance," *Appl. Opt.* **21**, 1686–1694 (1982).
15. J. H. T. Burke, O. Garcia, K. J. Hughes, B. Livedalen, and C. A. Sackett, "Compact implementation of a scanning transfer cavity lock," *Rev. Sci. Instrum.* **76**, 116105 (2005).
16. E. R. Peck and B. N. Khanna, "Dispersion of Nitrogen," *J. Opt. Soc. Am.* **56**, 1059–1063 (1966).
17. U. Griesmann and J. Burnett, "Refractivity of nitrogen gas in the vacuum ultraviolet," *Opt. Lett.* **24**, 1699–1701 (1999).
18. A. Buckingham and C. Graham, "The density dependence of the refractivity of gases," *Proc. R. Soc. A* **337**, 275–291 (1974).
19. J. Old, K. Gentili, and E. Peck, "Dispersion of carbon dioxide," *J. Opt. Soc. Am.* **61**, 89–90 (1971).
20. E. R. Peck and D. J. Fiisier, "Dispersion of argon," *J. Opt. Soc. Am.* **54**, 1362–1364 (1964).
21. J. Cariou and P. Luc, *Atlas du Spectre d'Absorption de la Molecule de Tellure* (Laboratoire Aime-Cotton, 1980), pp. 23.
22. T. J. Scholl, S. J. Rehse, R. A. Holt, and S. D. Rosner, "Absolute wave-number measurements in $^{130}\text{Te}_2$: reference lines spanning the 420.9–464.6 nm region," *J. Opt. Soc. Am. B* **22**, 1128–1133 (2005).